Spectral-Efficient and Power-Efficient MIMO-OFDM System with Time Diversity for Flat Fading Channel with Arbitrary Doppler Frequency Shift

Eman Zakaria [1,*], Ashraf Y. Hassan[1], H. EL Hennawy[2], and Abdelhady M. Abdelhady[1]

[1] Benha Faculty of Engineering, Electrical Engineering Department, Benha, Egypt
[2] Ain shams Faculty of Engineering, Electronics and Communications Department, Cairo, Egypt
Email: eman.zakeria@bhit.bu.edu.eg (E.Z.); Ashraf.fahmy@bhit.bu.edu.eg (A.Y.H.); Hadia.elhenawy@gmail.com (H.E.H.); Abdoeng78@gmail.com (A.M.A)
*Corresponding author

***Abstract*—In this work, a new method in time-diversity is used with an Orthogonal-Frequency-Division-Multiplexing (OFDM) system to enhance the bit-error-rate (BER) performance without increasing the signal bandwidth or decreasing the transmission rate. The diversity encoder is used to map the modulated symbols to diversity symbols for each OFDM subcarrier. The modulated symbol appears in N diversity symbols and it is transmitted on the same subcarrier through N different OFDM symbols. A Multiple-Input-Multiple-Output (MIMO) transmitter that works in spatial multiplexing mode, is used in this system to increase the spectral efficiency of the transmitted signal. The diversity gain of the proposed time-diversity method is equal to N that the order of the Walsh matrix. Symbols interleaving with programmable widths are used to get independent fading gain at arbitrary Doppler frequency shifts. The proposed system works in a flat fading channel with Doppler frequency shifts from 50 Hz to 7 kHz. In the receiver, a diversity decoder maps the vectors of diversity symbols to vectors of modulated symbols. The performance of the diversity decoder is the same as the performance of the Maximal-Ratio-Combiner (MRC) receiver. The proposed system increases the spectral efficiency of the transmitted signal and increases the Signal-to-Noise Ratio (SNR) of the decision variable by using time diversity without increasing the transmission bandwidth. The proposed system is simulated and implemented in FBGA. The performance of the implemented system is the same as the performance of the N channels diversity system with the Maximal-Ratio-Combiner (MRC) receiver.**

***Keywords*—time-diversity, diversity encoder, orthogonal-frequency-division-multiplexing system, maximal ratio combiner, multiple-input-multiple-output system, QR decomposition detector**

I. Introduction

The demand for wireless communications is constantly growing for high-data-rate transmissions to have better quality and coverage, be more bandwidth and power-efficient, and be deployed in diverse environments. Channel fading reduces the average Signal-to-Noise Ratio (SNR) of the received signal. It also distorts the transmitted signal causing Inter-Symbol Interference (ISI) among the received symbols. The improvement in SNR may not be achieved by higher transmit power or additional bandwidth. It is important to effectively reduce the effect of fading channels without additional power or extra bandwidth. A modern wireless system that uses Multiple-Input-Multiple-Output and Orthogonal-Frequency-Division-Multiplexing (MIMO-OFDM) is more popular because of its high transmission rate, its robustness against multipath fading, and its good spectral efficiency. This system achieves wide coverage and reliable communication. The recovery of the Channel State Information (CSI) accurately and the synchronization between the transmitter and receiver is the major challenge to the MIMO-OFDM system. Throughput gains and Quality of Service (QoS) improvements can be achieved with a proper combination of increased bandwidth, higher power efficiency, and a successful evolution of the networking architecture. In contrast, power-efficient and bandwidth-efficient have not seen any major improvements together in previous network generations. The aim of this work is to improve the signal transmission via flat fading channels by introducing a time-diversity system with moderated and high Doppler frequency shifts. In the introduced system, the transmitted symbol rate does not decrease due to the signal diversity method. Furthermore, the transmission bandwidth of the transmitted OFDM symbols does not change.

This paper is prepared as follows. Section II represents the literature review. Section III shows the time-diversity algorithm using diversity encoder and decoder, the transmitter structure and the mathematical model of the transmitted MIMO-OFDM symbols, the used channel model, the received signal model, and the structure of the receiver. The mathematical verification of the proposed time diversity system with the target diversity gain is also

Manuscript received August 8, 2023; revised August 30, 2023; accepted October 12, 2023; published February 10, 2024.

introduced in this section. In section IV, the simulation parameters and the specifications of the implemented system are represented. BER performance results of the simulated and real-time implemented system are presented at different SNRs. The real-time system is implemented and compared with the results of the MATLAB simulations and the theoretical results of the MRC receiver. Finally, the last section contains the Conclusions.

II. Literature Review

The MIMO system that has multiple transmitting antennas at one termination and multiple receiving antennas at the other termination are effectively combined to improve the channel capacity of the coverage area. In the OFDM system, multi-carrier modulation is used, where data is transmitted at a lower rate on each subcarrier using several orthogonal sub-carriers or sub-channels. The multipath effect can be eliminated by using OFDM technologies that transformed frequency selective channels into flat channels. Signal diversity is used to repeat the transmitted symbols in the receiver. The receiver uses these repeated with a signal-combining scheme to improve the received SNR [1, 2]. The signal diversity can occur in frequency, time and space. The time diversity involves sending the modulated symbol in different time slots to improve the reliability of the communication system. However, the rate of the transmitted symbol is decreased, and this also reduced the spectral efficiency of the received signal [3]. Frequency diversity reduces the transmission rate by sending the modulated symbol on several different carriers at once, however the additional transmission bandwidth also decreases the spectral efficiency of the received signal [4]. Space diversity, the modulated signals are sent and received using several transmitting antennas and various receiving antennas. Space diversity introduces interference among the sent symbols but neither increases the transmission bandwidth nor decreases the transmission rate [5]. To maintain the orthogonality of the transmitted signals in the time and spatial domains, space-time codes are used. Space-time codes maintain the received signal's spectral efficiency, but it complicates the transmitter and receiver structures [6]. Kannan and Kanniga [7] introduced ways to raise the performance in MIMO-OFDM systems such as channel selection, throughput, and Peak-to-Average Power Ratio (PAPR) reduction in networks to improve the reliability of the system and the spectral efficiency. Most of the research focuses on the successive-interference-cancelation OFDM (SIC-OFDM) to reduce the complexity and optimize the BER performance which both the basic requirements for SIC efficiency. Regarding BER performance and error resilience, the authors discussed the system's performance, robustness, dependability, and accuracy, therefore, it introduced the term Performance-Complexity Tradeoff [8].

In the literature of wireless communications, the frequency spectrum and power are the two main resource categories for the wireless electromagnetic medium. The trade-off between energy efficiency and bandwidth was researched in MIMO multi-carrier wireless networks and the effects of different numbers of antennas were investigated in [9]. Different types of power consumption models were considered in order to construct an appropriate closed-form approximation of the tradeoff between energy efficiency and spectrum efficiency over the MIMO Rayleigh fading channel [10]. Hu *et al.* [11] investigated to make MIMO-OFDM mobile multimedia communication systems more energy efficient. Yosef abd Hanzo [12] explored the characteristics and effects of the requirements for power versus bandwidth efficiency. They showed the bandwidth and the power efficiencies as a function of the SNR at the receiver. When the SNR increased, the bandwidth increased, and the power efficiency decreased. Ashraf [13] extended Shaping pulse is used to introduce a simple time-space diversity scheme for flat fading channels. Using one transmitting antenna, the system provides high gain in flat fading channels. In [14], One antenna is used to receive the transmitted signal in the new time diversity strategy that the author introduced to achieve time diversity in flat fading channels without increasing the data transmission rate. The suggested SISO system maintains the same bandwidth efficiency while achieving a high diversity gain. In order to obtain high diversity gain and increase bandwidth with spatial multiplexing, the time-diversity strategy is presented in this paper for MIMO systems. The Effect of Doppler Shift frequency on the performance of 2×2 MIMO-OFDM System is introduced in [15]. The massive MIMO reduce the Doppler effect in the OFDM system [16]. The doppler frequency is estimated for real time in FPGA [17–19].

III. Materials and Methods

In the proposed system, the power efficiency is increased by the time-diversity gain N, and the bandwidth efficiency is increased by the number of the transmitting antennas Mt. In the previous time-diversity systems [20–22], we cannot increase time-diversity gain without reducing the transmission rate. However, in the suggested system, the time-diversity gain can be increased without increasing the modulated symbols' transmission rate. The bandwidth of the transmitted OFDM symbols in this system does not influence by the used time-diversity system too. The bandwidth of the transmitted OFDM signal in this system is equivalent the bandwidth of the transmitted OFDM signal in the system without time diversity. Each transmitted OFDM signal has N modulated symbols, and ISI occurs among these. The diversity decoder is completely removed this ISI in the receiver. In this system, M diversity encoders are used before the OFDM modulator to implement the suggested time-diversity mechanism. The OFDM symbol has subcarrier number is M. A diversity encoder is added in the path of the modulated symbols of each OFDM subcarrier that introduced in [20]. The diversity encoder converts the modulated symbols of each subcarrier to diversity symbols. Every mapping cycle, the diversity encoder buffers a set of N-modulated symbols, and then it maps this set of modulated buffered symbols to a set of N-

diversity symbols. The time-diversity gain in the suggested system is represented by N. By changing the value of N, different diversity gains can be achieved. The diversity symbols will modulate the OFDM subcarriers instead of the modulated symbols. The diversity symbols N×M are transmitted by M OFDM subcarriers via N OFDM symbol periods. Each modulated symbol in the proposed system has a diversity period that is represented by the transmission period of the N OFDM symbols. This period must be more than the coherence time of the transmission channel to allow the diversity symbols to be affected by different independent fading gains. After the diversity encoder, symbols interleaving is used to distribute the diversity symbols, that produced from the same set of modulated symbols over various time intervals spaced with the coherence time of channel. The depth of the interleaving is equal to the diversity gain(N) and the width is equal to D that determined according to the fading channel coherence time. The time-diversity system does not change the rate of the modulated symbols since the transmission rate of the modulated symbols is equal to the diversity symbols' transmission rate. A MIMO transmitter that works in the spatial multiplexing mode, is added in the proposed system to improve the transmission rate of the OFDM symbols in the same transmission bandwidth. The spatial multiplexing MIMO transmission also increases the spectral efficiency of the transmitted time-diversity OFDM signal.

The receiver of the proposed system, a QR decomposition detector is used to demodulate the received MIMO-OFDM signal and extract the independent Mt OFDM symbols streams that are transmitted by the Mt transmitting antennas. An OFDM detector demodulates the M subcarriers in each OFDM stream and extracts M independent streams of diversity symbols. M blocks of symbols deinterleaving of length N and depth D are used to buffer the diversity symbols from each OFDM subcarrier. A diversity decoder maps back the N- diversity symbols in each column of the symbols deinterleaving to N-modulated symbols. The diversity decoder performs implicitly the function of the MRC receiver. Therefore, the SNR of the modulated symbols after the diversity decoder increases by the order of the used time-diversity system.

1) The mathematical model of the proposed MIMO-OFDM transmitter with time-diversity

Fig. 1 shows the block diagram of the transmitter. The incoming binary data symbols b_m are converted by using the QAM modulation into a string of complex modulated symbols g_m. These modulated symbols are changed from one serial stream to *M* (no. subcarriers) parallel streams using a serial-to-parallel converter.

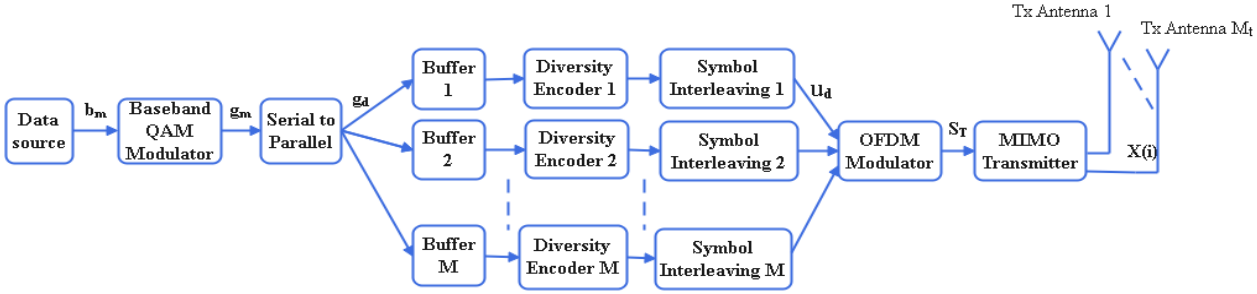

Fig. 1. The transmitter architecture of the time-diversity MIMO-OFDM system.

M buffers are used to collect the modulated symbols to the diversity encoders. The depth of each buffer is equal to *N (*the time diversity-gain as mentioned earlier). A diversity encoder converts the buffered *N* modulated symbols to *N* corresponding diversity symbols. There are M diversity encoders in the system. After the diversity encodes, the diversity symbols have M streams. The mapping process in the diversity encoder is done using an orthogonal Walsh matrix. Eq. (1) shows the mapping process inside the diversity encoder. u_{km}, is the k^{th} diversity symbol calculated by the m^{th} diversity encoder. *N* diversity symbols are calculated from the buffered *N* modulated symbols.

$$u_{km} = \sum_{n=1}^{N} W_{kn} \cdot g_{nm} \qquad 1 \le k \le \mathrm{N} \qquad (1a)$$

where N=4; $$W_{kn} = \begin{bmatrix} 1 & 1 & 1 & 1 \\ 1 & -1 & 1 & -1 \\ 1 & 1 & -1 & -1 \\ 1 & -1 & -1 & 1 \end{bmatrix} \qquad (1b)$$

g_{nm} is the n^{th} symbol in the set of buffered N modulated symbols in the m^{th} symbols stream. W_{kn} is the Walsh matrix (**W**) element in the k^{th} row and n^{th} column of the in-order *N*. W_{kn} is the coefficient that maps the n^{th} symbol in the buffered *N* modulated symbols to the k^{th} symbol in the N diversity symbols output set. The elements of the Walsh matrix take values from the set {–1, +1}. This matrix's rows and columns are orthogonal; therefore, the dot product is zero as Eq. (1b). The output symbols from the diversity encoder are interleaved using N×D symbols interleaving. The input symbols fill the interleaving matrix column-wise, and the output symbols are taken from the interleaving matrix row-wise. From Eq. (1), there are N diversity symbols for each modulated symbol at the output of the diversity encoder, so that performs intentional

interference among the modulated symbols. This interference should be able to be eliminated by the receiver. After the *M* diversity encoders and interleaving blocks, an OFDM modulator is used to map M diversity symbols (One diversity symbol from each diversity stream) to one OFDM symbol. In the OFDM symbol, each subcarrier transmits diversity symbols from the same diversity encoder. Since the subchannels of the OFDM symbol are assumed to be flat and the period of the OFDM symbol is smaller than or equal to the channel coherence time, the channel gain of each subcarrier should be constant for a minimum one OFDM symbol period. Therefore, the channel gains that affect the diversity symbols will be constant during at least one OFDM symbol period and not more than the *D* OFDM symbols period. The OFDM modulator and the diversity encoder distribute each modulated symbol over N OFDM symbols, whereas the diversity symbols from the same diversity encoder are broadcast on the same subcarrier in the OFDM symbol. Eq. (2) shows the generated OFDM symbol from the diversity symbols.

$$s_{kn} = \sum_{m=1}^{M} u_{km}.e^{j2\pi f_m n} \ , 1 \leq \ n \leq \mathrm{M} \qquad (2)$$

s_{kn} is the k^{th} OFDM symbol's n^{th} sample. The number of samples in the OFDM symbols is equivalent to M. u_{km} is the k^{th} diversity symbols in the m^{th} stream of diversity symbols, which modulates the m^{th} subcarrier. If we have N×M modulated symbols. These symbols will be mapped to N×M diversity symbols using the Walsh matrix as in Eq.1. The OFDM modulator will generate N OFDM symbols with M subcarrier as shown in Eq. (3).

$$\mathbf{S} = \mathbf{U}^T.\mathbf{F} \qquad (3a)$$

$$\begin{bmatrix} s_{11} & s_{12} & \dots & s_{1M} \\ s_{21} & s_{22} & \dots & s_{2M} \\ \vdots & \vdots & \ddots & \vdots \\ s_{N1} & s_{N2} & \dots & s_{NM} \end{bmatrix} = \begin{bmatrix} u_{11} & u_{12} & \dots & u_{1M} \\ u_{21} & u_{22} & \dots & u_{2M} \\ \vdots & \vdots & \ddots & \vdots \\ u_{N1} & u_{N2} & \dots & u_{NM} \end{bmatrix}. \begin{bmatrix} 1 & e^{j2\pi f_1} & e^{j4\pi f_1} & e^{j6\pi f_1} & \dots & e^{j2\pi f_1 N} \\ 1 & e^{j2\pi f_2} & e^{j4\pi f_2} & e^{j6\pi f_2} & \dots & e^{j2\pi f_2 N} \\ \vdots & \vdots & \vdots & \vdots & \ddots & \vdots \\ 1 & e^{j2\pi f_M} & e^{j4\pi f_M} & e^{j6\pi f_M} & \dots & e^{j2\pi f_M N} \end{bmatrix} \qquad (3b)$$

S is a matrix of N OFDM symbols. Each row in ***S*** represents an OFDM symbol of M samples. **U** is a matrix of diversity symbols. The m^{th} row in **U** represents the *N* diversity symbols that are produced from the m^{th} diversity encoder and modulate the m^{th} subcarrier. **F** is the IFFT mapping matrix. Each row in **F** represents the samples of one subcarrier in one OFDM symbol. A cyclic prefix of *P* samples is added in the front of each OFDM symbol to prevent ISI. It is also used for the synchronization purpose with OFDM symbols. The length of the cyclic prefix depends on the channel's multipath delay. Eq. (4) shows the matrix $\boldsymbol{S_T}$ of the OFDM symbols after adding the cyclic prefix.

$$\mathbf{S_T} = [\mathbf{S_{cp}}|\mathbf{S}] = \begin{bmatrix} s_{1P} & \dots & s_{1M} \\ s_{2P} & \dots & s_{2M} \\ \vdots & \ddots & \vdots \\ s_{Np} & \dots & s_{NM} \end{bmatrix} \begin{bmatrix} s_{11} & s_{12} & \dots & s_{1M} \\ s_{21} & s_{22} & \dots & s_{2M} \\ \vdots & \vdots & \ddots & \vdots \\ s_{N1} & s_{N2} & \dots & s_{NM} \end{bmatrix} \qquad (4)$$

The symbols rate R_s at the output of the OFDM modulator is equivalent to M×R_o, where R_o is the OFDM symbols rate. R_o is also equal to the spacing between the OFDM subcarriers. The symbols rate R_s in the proposed time-diversity system is alike the symbols rate in conventional systems without diversity encoder, i.e., time-diversity isn't used. Therefore, the time diversity in the proposed system neither increase the symbols' transmission rate nor additional the transmission bandwidth.

The ratio between the symbols' transmission rate and the transmission bandwidth is defined as spectral efficiency. The number of subcarriers (*M*), the OFDM symbols rate (R_o), and the roll-off factor (α_{roll}) of the used shaping pulse (the shaping factor of the transmitting filter) effect on the bandwidth of the OFDM signal. The OFDM signal's bandwidth in this system is equal to $(\mathrm{M} + \alpha_{roll}) \times R_o$. When Nyquist pulse is used, the roll-off factor is zero, however, when full raised-cosine pulse is used, the roll-off factor is one. The spectral efficiency of the suggested time-diversity system after the OFDM modulator is shown in Eq. (5) [23].

$$\eta_{Bw} = \frac{\mathrm{M} \times R_o}{(\mathrm{M} + \alpha_{roll}) \times R_o} = \frac{\mathrm{M}}{(\mathrm{M} + \alpha_{roll})} \qquad (5)$$

In the proposed system, MIMO transmission is used in the spatial multiplexing mode to increase the OFDM symbols transmission rate and thus increase the spectral efficiency. The number of transmitting antennas in the MIMO transmitter is M_t. The total transmission rate will be M_t×R_o OFDM symbols per second, which is equal to M_t×M×R_o modulated symbols per second. The new spectral efficiency will be equal to:

$$\eta_{Bw} = \frac{\mathrm{M}_t \times \mathrm{M}}{(\mathrm{M} + \alpha_{roll})} \qquad (6)$$

The transmitted MIMO vector is shown in Eq. (7). $\mathbf{X}(i)$ is the i^{th} MIMO symbol (vector). $\mathbf{S}_{\mathbf{T},\mathrm{M_t}*i+j}$ is the OFDM symbol in the row number $(\mathrm{M}_t * i + j)$ in the OFDM matrix shown in Eq. (4).

$$\mathbf{X}(i) = \begin{bmatrix} \mathbf{S}_{\mathbf{T},\mathrm{M_t}*i+1} \\ \mathbf{S}_{\mathbf{T},\mathrm{M_t}*i+2} \\ \vdots \\ \mathbf{S}_{\mathbf{T},\mathrm{M_t}*i+\mathrm{M_t}} \end{bmatrix} \qquad (7)$$

2) The receiver structure of the time-diversity MIMO-OFDM

The presented time-diversity system is designed for frequency non-selective fading channels with arbitrary Doppler frequency shifts. The OFDM symbol rate R_o, which is equivalent to the channel spacing between the subcarriers in the OFDM symbol, is assumed to be less than or equivalent to the coherence bandwidth of the

channel. The OFDM symbol rate R_o should be equal to the Doppler frequency (the reciprocal of the channel coherence time) to have independent channel gain in each OFDM symbol. According to the measurements in [16], if the system works in the 5 GHz band, the worst-case coherence bandwidth is 20 kHz. It is greater than the Doppler frequency for relative speeds smaller than 1000 km/h. The diversity symbols in each OFDM subcarrier will not have different independent channel gains during successive OFDM periods if the length of these periods is smaller than the coherence time of the channel. Therefore, symbols interleaving is used in the transmitter. The width of the symbols interleaving is equal to the rate of the OFDM symbol divided by the Doppler frequency shift. Therefore, the diversity symbols in each row experience the same fading gain, however, the diversity symbols in each column experience different independent fading gains. The width of the symbols interleaving in the proposed system is programable and it depends on the relative speed between the transmitter and the receiver. To maintain the target transmission rate of OFDM symbols when the coherence bandwidth of the channel becomes smaller, the number of subcarriers is increased to compensate for the decrease in the OFDM symbols' transmission rate. Typical numerical data will be represented in the simulation section. Fig. 2 shows the block diagram of the proposed receiver. It involves of the MIMO detector, the OFDM demodulator, the diversity decoder plus symbols combining, and the baseband QAM demodulator. The synchronization and channel estimation topics will be treated in another work and they are out of the scope of this paper. Now, it is expected that the receiver has the channel status information (CSI). The receiver has M_r receiving antennas. M_r must be greater than or equivalent to the number of the transmitting antennas M_t to achieve the required transmission capacity. Moreover, the spacing between the transmitting antennas and between the receiving antennas must be multiple of the wavelength of the transmitted wave to have independent channel gain between each pair of the transmitting and receiving antennas [17]. Eq. (8) shows the received MIMO symbol $\mathbf{Z}(i)$ from the receiving antennas at the i^{th} MIMO symbol.

$$\mathbf{Z}(i) = \mathbf{H}(i).\mathbf{X}(i) + \mathbf{W}_{noise} \tag{8}$$

$\mathbf{H}(i)$ is the channel matrix of M_r rows and M_t columns at the i^{th} MIMO symbol. It is assumed that the channel matrix's components are complex, zero-mean Gaussian random variables. The real and imaginary parts of the channel gains have the same variance. The estimation of the channel is excluded in this work. $\mathbf{W}_{noise}$ is the white Gaussian noise matrix. It has M_r rows and M_t columns too. The noise samples have zero mean and σ^2 variance. Eq. (9) shows the noise covariance matrix.

$$cov[\mathbf{W}_{noise}] = E[\mathbf{W}_{noise}^{H}.\mathbf{W}_{noise}] = \sigma^2\mathbf{I} \tag{9}$$

$\mathbf{I}$ is the unity matrix. $(.)^H$ is the conjugate transpose of the matrix.

Since the MIMO decoding and the OFDM demodulation are linear operations, their locations can be swapped in the proposed receiver. We can start the signal processing in the receiver with the OFDM demodulation and after that, the MIMO detector is used. This simplifies the implementation complexity. If the MIMO detector comes first, the input MIMO vector will be a matrix of M_r OFDM symbols with M time-domain samples. Each column vector consists of M_r samples in time-domain of the interfered M_t OFDM symbols. On the other hand, when the OFDM demodulator comes first, the input to the MIMO detector will be a matrix of M_r OFDM symbols with M frequency domain samples. Each column vector consists of M_r complex diversity symbols that modulate a certain subcarrier in the OFDM symbol.

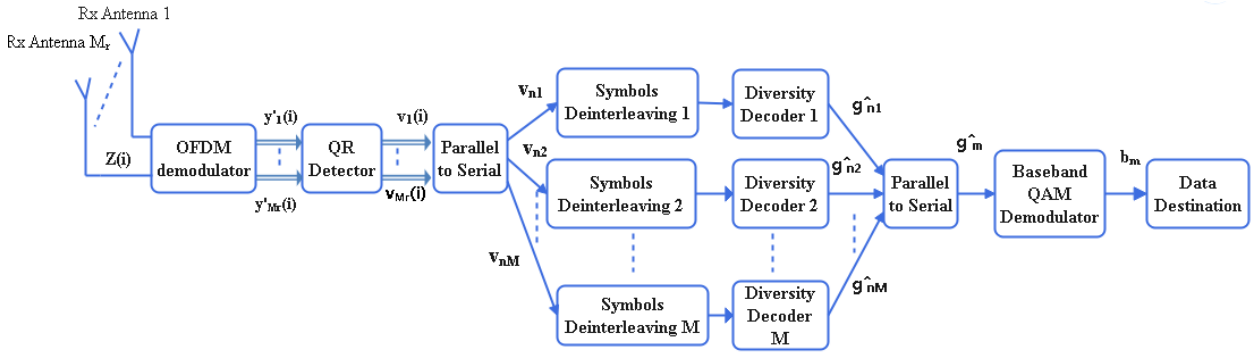

Fig. 2. The receiver architecture of the time-diversity MIMO/OFDM system.

The subcarrier index is equivalent to the column index in the input matrix to the MIMO detector.

a) The OFDM demodulator

The OFDM demodulator converts vectors of M time-domain samples of the received OFDM symbols to vectors of M frequency-domain samples. Each sample in the frequency domain vector represents a diversity symbol that modulates the subcarrier corresponding to the index of that frequency sample. When OFDM modulation is used with MIMO transmission in spatial multiplexing mode, the story is different. M_r OFDM demodulators are used to convert the time-domain OFDM symbols received by the M_r receiving antennas to M_r vectors of M frequency-domain samples. Each sample in the frequency vectors is the sum of the diversity symbols that modulate the subcarriers corresponding to the index of this frequency sample and were transmitted by the M_t transmitting antennas with different channel gains. The block diagram of the OFDM demodulator is shows in Fig.

3 The OFDM demodulator involves of three parts. The cyclic prefix remover is the first part. In this part, the demodulator synchronizes with the OFDM symbol delimiters.

The cyclic prefix samples are specified and removed from the received OFDM symbols before applying them to the FFT algorithm in the next part. The second part of the demodulator is the FFT part. It receives M time-domain samples per OFDM symbol from the preceding part and applies the FFT algorithm to get the M frequency domain samples. Since the proposed system works in channels with arbitrary Doppler frequency shifts from 50 Hz to 7 kHz, the received OFDM symbols will be afflicted with inter-carrier interference (ICI). Due to the Doppler frequency shift, the orthogonality between the received OFDM subcarriers is lost. Therefore, the diversity symbols on these subcarriers overlap each other. A decorrelator detector is used in the last part of the OFDM demodulator to remove this ICI. The decorrelator detector increases the frequency domain vector of M samples from the FFT part with the inverse of the subcarriers' correlation matrix $\mathbf{R}_{SC}$. The elements of the subcarriers' correlation matrix are the correlation coefficients between the received subcarriers with Doppler frequency shift f_d and the transmitted subcarriers without Doppler frequency shift. Eq.10 shows the correlation element ρ_{ij} in the i^{th} row and j^{th} column of the subcarriers' correlation matrix $\mathbf{R}_{SC}$, which is the correlation between the received j^{th} subcarrier with Doppler frequency shift and the transmitted i^{th} subcarrier with no Doppler frequency shift.

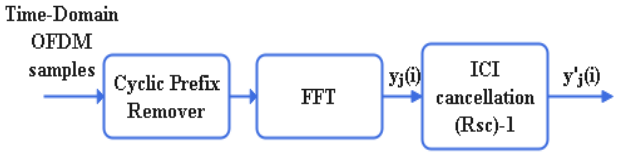

Fig. 3. The OFDM demodulator in the time-diversity MIMO/OFDM system.

$$\rho_{ij} = \frac{1}{\mathrm{M}} \sum_{m=1}^{M} e^{-j2\pi f_i m} . e^{j2\pi (f_j + f_d) m} \quad (10)$$

The row OFDM vector $\boldsymbol{y_j}(i)$ at the output of the FFT algorithm in the j^{th} OFDM demodulator at the i^{th} MIMO transmission period is shown in Eq. (11).

$$\boldsymbol{y_j}(i) = [h_{j1}(i)\ \ h_{j2}(i)\ \ \dots\ \ h_{jM_t}(i)]$$

$$\begin{bmatrix} u_{11}(i) & u_{12}(i) & \dots & u_{1M}(i) \\ u_{21}(i) & u_{22}(i) & \dots & u_{2M}(i) \\ \vdots & \vdots & \ddots & \vdots \\ u_{M_t1}(i) & u_{M_t2}(i) & \dots & u_{M_tM}(i) \end{bmatrix} \begin{bmatrix} \rho_{11} & \rho_{12} & \dots & \rho_{1,M} \\ \rho_{21} & \rho_{22} & \dots & \rho_{2,M} \\ \vdots & \vdots & \ddots & \vdots \\ \rho_{M,1} & \rho_{M,2} & \dots & \rho_{M,M} \end{bmatrix} + \mathbf{W`} \quad (11)$$

$h_{jl.}(i)$ is the gain of the complex channel from the l^{th} transmitting antenna to the j^{th} receiving antenna at the i^{th} MIMO symbol transmission. $u_{lm}(i)$ is the diversity symbol that is transmitted on the m^{th} subcarrier by the l^{th} transmitting antenna at the i^{th} MIMO symbol transmission.

$\mathbf{W`}$ is the matrix of white Gaussian noise samples. It has $M_t$ rows and M columns. The noise samples in $\mathbf{W`}$ have σ^2 variance and zero mean. The row vector $\boldsymbol{y_j}(i)$ is multiplied by the inverse of the correlation matrix $\mathbf{R}_{SC}$ to remove the ICI as shown in Eq. (12).

$$\boldsymbol{y`_j}(i) = \mathbf{R}_{SC}^{-1} . \boldsymbol{y_j}(i) = [h_{j1}(i)\ \ h_{j2}(i)\ \ \dots\ \ h_{jM_t}(i)].$$
$$\begin{bmatrix} u_{11}(i) & u_{12}(i) & \dots & u_{1M}(i) \\ u_{21}(i) & u_{22}(i) & \dots & u_{2M}(i) \\ \vdots & \vdots & \ddots & \vdots \\ u_{M_t1}(i) & u_{M_t2}(i) & \dots & u_{M_tM}(i) \end{bmatrix} + \mathbf{W`} . \mathbf{R}_{SC}^{-1} \quad (12)$$

Eq. (12) shows the OFDM row vector $\boldsymbol{y`_j}(i)$ the output of the j^{th} OFDM demodulator at the i^{th} MIMO transmission period after removing the ICI. The m^{th} sample in this row vector is the sum of the M_t diversity symbols that modulate the m^{th} subcarrier in the M_t OFDM symbols transmitted by the M_t transmitting antennas in the i^{th} MIMO symbol. Eq. (13) shows the noise's covariance matrix component in the OFDM vector $\boldsymbol{y`_j}(i)$.

$$cov[\mathbf{W`} . \mathbf{R}_{SC}^{-1}] = E\left[ \left( \mathbf{W`} . \mathbf{R}_{SC}^{-1} \right)^H . \mathbf{W`} . \mathbf{R}_{SC}^{-1} \right] = \sigma^2 \mathbf{R}_{SC}^{-2} \quad (13)$$

In Eq. (14), the matrix $\mathbf{Z}(i)$ of the M_r rows vectors $\boldsymbol{y`_j}(i)$ is the input to the MIMO detector. The samples in the j^{th} row of $\mathbf{Z}(i)$ are the output frequency-domain samples from the j^{th} OFDM demodulator after removing the ICI. The algorithm of the MIMO detector will work on the samples of the matrix $\mathbf{Z}(i)$ column-wise because each column carries interfering symbols that modulated the same subcarrier.

$$\mathbf{Z}(i) = \begin{bmatrix} \boldsymbol{y`_1}(i) \\ \boldsymbol{y`_2}(i) \\ \vdots \\ \boldsymbol{y`_{M_r}}(i) \end{bmatrix} = \begin{bmatrix} y`_{11}(i) & y`_{12}(i) & \dots & y`_{1M}(i) \\ y`_{21}(i) & y`_{22}(i) & \dots & y`_{2M}(i) \\ \vdots & \vdots & \ddots & \vdots \\ y`_{M_r,1}(i) & y`_{M_r,2}(i) & \dots & y`_{M_r,M}(i) \end{bmatrix} \quad (14)$$

b) The MIMO detector

The OFDM symbols in the received MIMO symbols interfere with each other as shown in Eq. (11)–(12). To remover this interference, a QR detector is used. The QR detector decomposes the channel matrix $\mathbf{H}(i)$ into $\mathbf{Q}(i)$ (an orthogonal matrix) and $\mathbf{R}(i)$(an upper triangle matrix). The $\mathbf{Q}(i)$ is a square matrix of M_r rows. The $\mathbf{R}(i)$ matrix has M_r rows and M_t columns. The number of independently resolvable paths in the channel is equal to M_t since M_t is smaller than M_r. Therefore, the number of non-zero rows in $\mathbf{R}(i)$ is equal to M_t.

The QR detector multiplies the input MIMO matrix $\mathbf{Z}(i)$ with the inverse of the $\mathbf{Q}(i)$ matrix ($\mathbf{Q}^{-1}(i) = \mathbf{Q}(i)$ because the matrix is orthogonal). The output matrix $\mathbf{Z`}(i)$ after matrix multiplication is shown in Eq. (15).

$$\mathbf{Z`}(i) = \mathbf{Q^{-1}}(i) . \mathbf{Z}(i)$$

$$= \mathbf{R}(i).\mathbf{U}(i) + \mathbf{Q^{-1}}(i).\mathbf{W`}.\mathbf{R_{SC}^{-1}} \quad (15)$$

The matrix multiplication in Eq.15 does not affect the noise power since $\mathbf{Q}(i)$ is an orthogonal matrix. Eq.16 shows the noise samples' covariance-matrix after multiplying the input noise matrix $\mathbf{W`}$ with the inverse of the $\mathbf{Q}(i)$ matrix.

$$cov[\mathbf{Q^{-1}}(i).\mathbf{W`}.\mathbf{R_{SC}^{-1}}] = E[\mathbf{R_{SC}^{-1}}.\mathbf{W`}^{H}.\mathbf{Q}_i(i).\mathbf{Q^{-1}}(i).\mathbf{W`}.\mathbf{R_{SC}^{-1}}] = \sigma^2\mathbf{R_{SC}^{-2}} \quad (16)$$

After multiplying the received MIMO matrix with the inverse of the $\mathbf{Q}(i)$ matrix, a backpropagation search algorithm is applied to each column vector in $\mathbf{Z`}(i)$ to get an estimation for the scaled diversity symbols $u_{lk}(i)$. The estimation of the diversity symbol that modulates the m^{th} subcarrier in the j^{th} OFDM symbol in the receiver i^{th} MIMO vector is calculated by Eq. (17).

$$v_{jm}(i) = \boldsymbol{Z`}_{jm}(i) - \sum_{l=M_t}^{j+1} \frac{r_{lm}(i).v_{lm}(i)}{r_{ll}(i)} + q_{jm} \quad (17)$$

q_{jm} is the AWGN sample that is added to the m^{th} diversity symbol $v_{jm}(i)$ in the j^{th} OFDM symbol. $r_{lm}(i)$ is the complex gain of the m^{th} diversity symbol in the j^{th} OFDM symbol at the i^{th} MIMO symbol. $r_{lm}(i)$ is also the element in the l^{th} row and m^{th} column of the upper triangle matrix $\mathbf{R}(i)$. Eq.18 shows the comparable mathematical model for the estimated diversity symbol at the QR detector's output.

$$v_{jm}(i) = \alpha_{jm}(i).u_{jm}(i) + q_{jm} \quad (18)$$

$\alpha_{jm}(i)$ is the complex gain of the m^{th} diversity symbol $u_{jm}(i)$ in the j^{th} OFDM symbol. The MIMO detector's output is a vector of M_t OFDM symbols, each of them contains M frequency samples modulated with M diversity symbols. The parallel OFDM symbols are converted to a serial stream of OFDM symbols with the same order used in the transmitter as shown in Eq.7. The OFDM symbols at the output of the MIMO detectors are in the frequency domain. The symbol that modulates the m^{th} subcarrier in the n^{th} OFDM symbol is shown in Eq. (19).

$$v_{nm} = \alpha_{nm}.u_{nm} + q_{nm}, \qquad n = i \times \mathrm{M}_t + j \quad (19)$$

c) The diversity decoder and symbols combining

This part of the receiver is responsible for two tasks. The first task is the decoding of the estimated diversity symbols back to modulated symbols. Secondly is the combining of the modulated symbols with different channel gains in one decision value. This part of the receiver implicitly performs these two tasks simultaneously. The first stage in this part is the diversity symbols deinterleaving. The deinterleaving matrix's size is equal to the size of the interleaving matrix. It has N rows and D columns. The diversity symbols from the MIMO detector fill the deinterleaving matrix row-wise and the output symbols are taken from this matrix column-wise. As mentioned earlier, the process of the diversity symbols interleaving guarantees that the N diversity symbols got in the columns of the deinterleaving matrix are affected by different independent channel gains. The estimations of the diversity symbols are calculated from Eq. (19) by multiplying v_{nm} with the reciprocal of the complex gain α_{nm} as shown in Eq. (20).

$$\hat{u}_{nm} = \frac{1}{\alpha_{nm}} v_{nm} = u_{nm} + \frac{q_{nm}}{\alpha_{nm}} \quad (20)$$

The estimations of the diversity symbols from the m^{th} subcarrier create a stream of symbols corresponding to the diversity symbols stream that modulates this subcarrier in the transmitter. M blocks of symbols deinterleaving are used to collect the estimated diversity symbols stream from the M subcarrier to the M diversity decoders. The diversity decoders read the estimated diversity symbols in the columns of the deinterleaving matrices and make the inverse function of the diversity encoders. Each diversity decoder converts the *N* diversity symbols in each column of its deinterleaving matrix to *N* estimations of modulated symbols. The same Walsh matrix used in the transmitter is also used here to remap the buffered estimated diversity symbols to estimated modulated symbols. The k^{th} estimated modulated symbol $\hat{g}_{km}$ in the m^{th} stream of estimated modulated symbols is shown in Eq. (21).

$$\hat{g}_{km} = \sum_{n=1}^{N} W_{kn}.\hat{u}_{nm} = N.g_{km} + \sum_{n=1}^{N} W_{nk}.\frac{q_{nm}}{\alpha_{nm}} \quad ,1 \le k \le \mathrm{N} \quad (21)$$

In Eq.21, the decision variable $\hat{g}_{km}$ is the MRC of the k^{th} symbol in the m^{th} stream of estimated modulated symbols. The diversity decoder merges the same modulated symbols from N diversity symbols that were transmitted in successive N OFDM symbols on the same subcarrier. As mentioned earlier, the diversity decoder performs the function of the MRC in the proposed receiver as well as converts the estimated diversity symbols to estimated modulated symbols.

In the classical MRC receiver, the combiner receives N different decision variables for the same symbol from the demodulator. These N decision variables come from N independent channels with N different gains. Eq. (22) shows the outputs from the demodulator (the decision variables) in an MRC receiver.

$$\begin{aligned} r_{k1} &= \alpha_{k1}.g_k + w_{k1} \\ r_{k2} &= \alpha_{k2}.g_k + w_{k2} \\ &\vdots \\ r_{kN} &= \alpha_{kN}.g_k + w_{kN} \end{aligned} \quad (22)$$

g_k is the k^{th} modulated symbol. The complex gain in the n^{th} channel path is α_{kn}. w_{kn} is the AWGN component. r_{kn} is the n^{th} demodulator output. The MRC receiver combines the N decision variables in Eq. (22) in one decision variable as shown in Eq. (23).

$$\hat{g}_k^{MRC} = \sum_{n=1}^{N} \frac{r_{kn}}{\alpha_{kn}} = \mathrm{N}.g_k + \sum_{n=1}^{N} \frac{w_{kn}}{\alpha_{kn}} \quad (23)$$

By comparing Eq. (21) and Eq. (23), we come to the conclusion that, if the mapping coefficients $W_{nk}$are from the set {−1,+1}, the output of the diversity decoder in the proposed receiver is similar to the output of the MRC receiver with independently N fading channels.

d) The QAM baseband detector

This is the last part of the proposed receiver. Before the baseband demodulation, the parallel symbols from the outputs of the M diversity decoders are converter to a serial stream of estimated modulated symbols using a parallel-to-serial converter. The modulated symbols are divided by N to conserve the power of the used QAM signal constellation. The QAM detector uses the maximum likelihood (ML) algorithm to demodulate the estimated complex QAM symbols at its input to binary symbols at its output.

IV. Result and Discussion

In this section, the proposed MIMO-OFDM system's system specifications, simulation findings, and implementation results are represented. The MIMO's spatial multiplexing factor of the used system is 2 OFDM symbols per one MIMO symbol since two transmitting antennas are used in the proposed system. The transmitted OFDM symbols has 5 GHz carrier frequency. It is assumed that the channel model is frequency selective for the whole bandwidth of the OFDM signal. But for each subchannel in the OFDM signal, the channel model is flat-fading channel with arbitrary Doppler frequency in the range started from 50 Hz (maximum relative speed equal to 10.8 Km/h) to 7 kHz (maximum relative speed equal to 1500 Km/h). The worst-case coherence bandwidth of the used wireless channel is equal to 20 kHz, therefore, the rate of the OFDM symbol is 20 k baud and the OFDM subcarriers' spacing is equal to 20 kHz too. The channel gain in each subchannel is assumed as complex Gaussian random variable. The modulation scheme in each subcarrier is 16-QAM. The number of subcarriers in the implemented system is not fixed and can be configured according to the target information rate. Table I shows the used number of subcarriers and the target information rate for each number when 16-QAM modulation is used. 32 pilot symbols per OFDM symbol are used for synchronization and channel estimation. The transmit filter roll-off factor is equal to 0.15. Table I shows the bandwidth and the spectral efficiency of the transmitted OFDM symbols.

TABLE I. The Information Rates in the Implemented Systems

Bandwidth	Number of subcarriers	Information rate	Spectral efficiency
5.123 MHz	256	35.84 Mbps	6.996 bits/s/Hz
10.243 MHz	512	76.80 Mbps	7.498 bits/s/Hz

As shown before, the width D of the interleaving matrix and the deinterleaving matrix is not fixed and is determined according to the coherence time or the largest Doppler frequency shift in the fading channel. The largest coherence time of the channel determines the maximum value of *D* (corresponding to the minimum doppler frequency shift). Since the OFDM symbol rate is 20 k baud, the OFDM symbol period is 50 μs. The maximum coherence-time is equal to 20 ms, which corresponds to 50 Hz Doppler-frequency shifts. Therefore, D_{max}= 400 diversity symbols. The smallest coherence time of the channel determines the minimum value of D (corresponding to the largest doppler-frequency shift). The minimum coherence time is equal to 142.85 μs, which corresponds to 7 kHz Doppler frequency shift. Therefore, D_{min}= 3 diversity symbols. The implemented widths of the interleaving and deinterleaving matrices are 400, but the physical layer controller will use portions of these widths according to the estimated channel's coherence time. The implemented system achieves the target diversity gain (N) for arbitrary Doppler frequency shifts from 50 Hz to 7 kHz.

Matlab m-file scripts are used to simulate the proposed system. The BER in the simulated system is compared with the BER of the optimum MRC receiver at different diversity gains. Walsh matrices that used in the diversity encoder of the simulated system in order N equal to 2,4,8, and 16. The gain of the time-diversity in the simulated system is equal to the order of the used Walsh matrices. The propagation channel that used is the flat fading Rayleigh channel model. The system is simulated also with different Doppler frequency shifts from 50 Hz to 7 kHz.

Fig. 4 shows the results of the average BER in the data that received from the proposed receiver once the Doppler frequency shift in the channel is 50 Hz. As it can be seen, the performance of the proposed system's BER is a little less than the performance of the MRC receiver's BER. The SNR difference between these systems is less than 0.5 dB at the same BER value. The reason for this difference is the enhancement of the noise of the decorrelator detector in the ICI removal stage of the OFDM demodulator. This average SNR difference increases as the Doppler frequency shift increases, since the noise enhancement of the detector increases when the correlation between the subcarriers increases. The correlation between the subcarrier increases when the channel's Doppler frequency shift increases.

Fig. 5 shows that the SNR difference between the BER performance of the MRC and the BER performance of the proposed system increases to 2dB with the Doppler frequency shift is 7 kHz. The average BER in the output of the proposed system is simulated at different average SNRs and Doppler frequency shifts. The simulated results are represented in Figs. 6–9. The figures show that the average BER decreases as the Doppler frequency shift increases. Moreover, it is found that the reduction rate in the average BER decreases when the average SNR increases. The reason for this result is that the enhancement in the noise of the decorrelator detector in the ICI removal stage is small at a high average SNR.

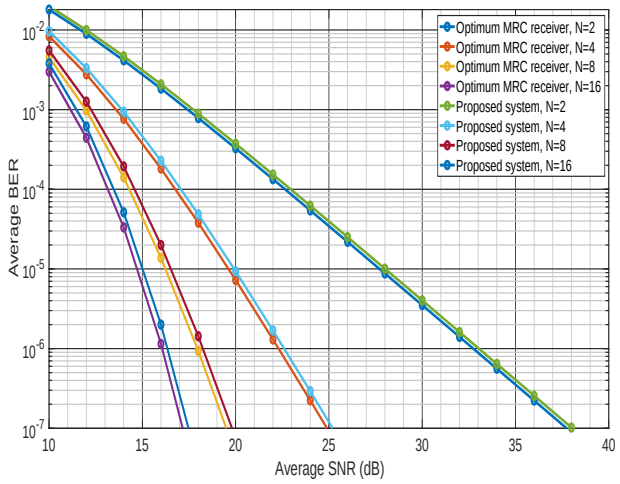

Fig. 4. A comparison between the proposed system's BER and the N channels MRC receiver's BER at flat Rayleigh fading channel with 50 Hz Doppler frequency Shift, BW=5.123 MHz, No. of subcarriers=256, rate=35.84 Mbps and Spectral efficiency=6.996 bits/s/Hz.

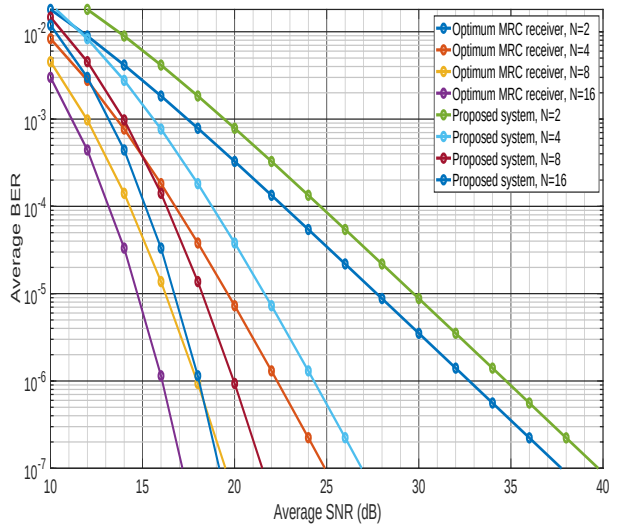

Fig. 5. A comparison between the proposed system's BER and N channels MRC receiver's BER at flat Rayleigh fading channel with 7 kHz Doppler frequency shift, BW=5.123 MHz, No. of subcarriers=256, rate=35.84 Mbps and Spectral efficiency=6.996 bits/s/Hz.

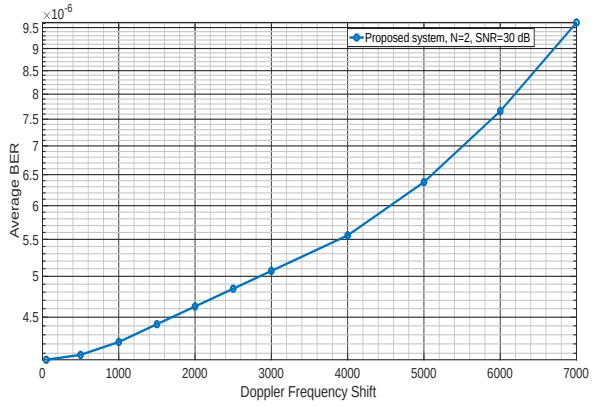

Fig. 6. The variation of the proposed system's BER with the Doppler frequency shift at SNR = 30 dB, N = 2, BW=5.123 MHz, No. of subcarriers=256, rate=35.84 Mbps and Spectral efficiency=6.996 bits/s/Hz.

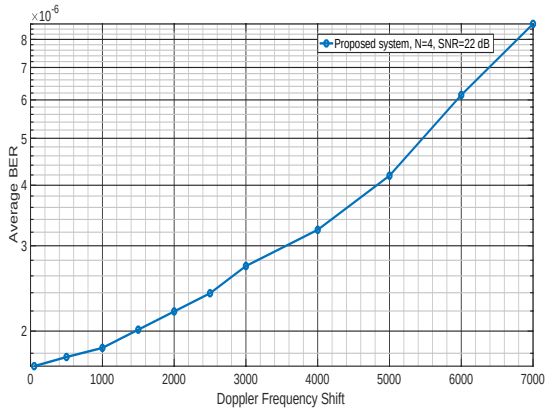

Fig. 7. The variation of the proposed system's BER with the Doppler frequency shift at SNR = 22 dB, N = 4, BW=5.123 MHz, No. of subcarriers=256, rate=35.84 Mbps and Spectral efficiency=6.996 bits/s/Hz.

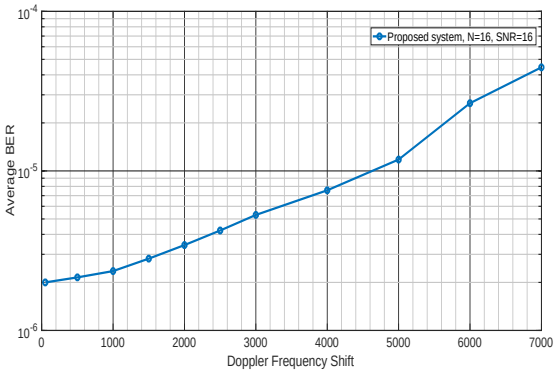

Fig. 8. The variation of the proposed system's BER with the Doppler frequency shift at SNR = 16 dB, N = 16, BW=5.123 MHz, No. of subcarriers=256, rate=35.84 Mbps and Spectral efficiency=6.996 bits/s/Hz.

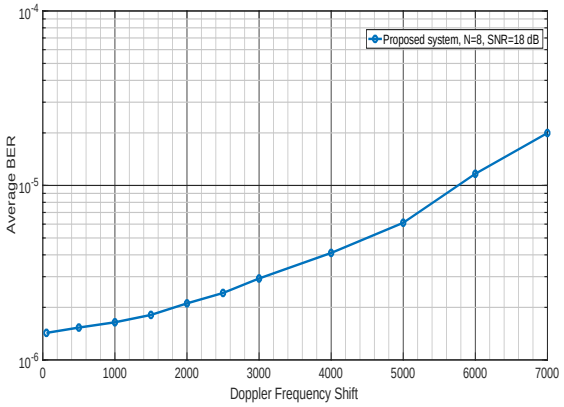

Fig. 9. The variation of the proposed system's BER with the Doppler frequency shift at SNR = 18 dB, N = 8, BW=5.123 MHz, No. of subcarriers=256, rate=35.84 Mbps and Spectral efficiency=6.996 bits/s/Hz.

This is a feature of the decorrelator detector. Consequently, the decrease rate in the average BER of the proposed system with Doppler frequency shift is inversely proportional to the average SNR.

The proposed system is also simulated at the lowest Doppler frequency shift and the average noise power of the decision variable after the diversity decoder is calculated. This simulation case is done to compare the

signal combining effect in the proposed diversity decoder with that of the MRC receiver, which is the optimal signal combining method. The simulated results of this case are presented in Fig. 10. The results in Fig. 10 match the accomplished mathematical result. The diversity decoder's output decision variable's average noise power is practically identical to the MRC receiver's output decision variable's average noise power. Therefore, the signal combining that is done inside the diversity decoder is the same as the signal combining in the MRC receiver.

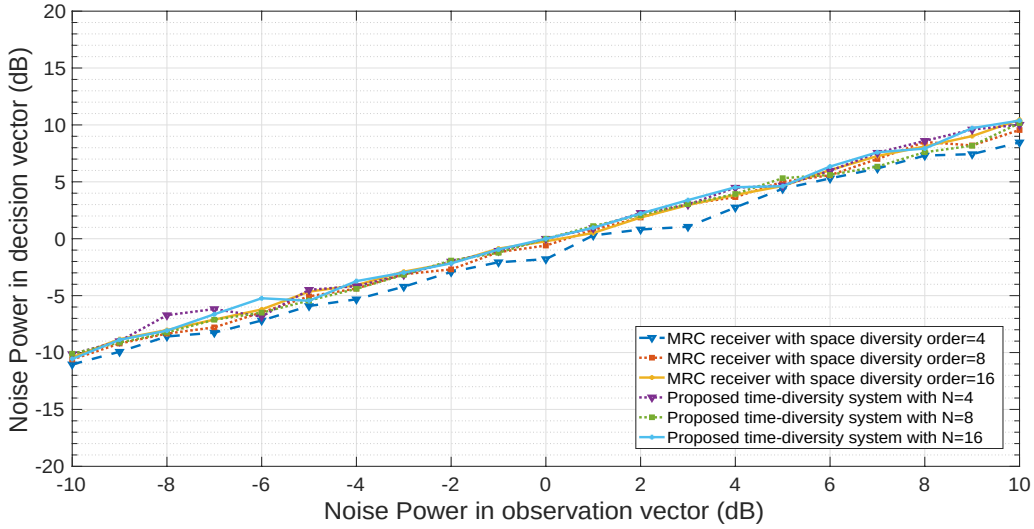

Fig. 10. A comparison between the noise power in the observation vector and the noise power in the decision vector for different configurations of the proposed system and N channel MRC receiver, BW=5.123 MHz, No. of subcarriers=256, rate=35.84 Mbps and Spectral efficiency=6.996 bits/s/Hz.

Fig. 11 shows that the SNR difference between the performance of the MMSE's BER and the performance of the proposed system's BER. The maximum ratio combiner (MRC) is optimum in the point-to-point transmission; however, the channel estimation of MMSE is better than MRC in multi-user system. In this system, MRC is used to transmit the data from point to point. A comparison between the noise power in the observation vector and the noise power in the decision vector for different configurations of the proposed system and N channel MMSE receiver is shown in Fig. 12.

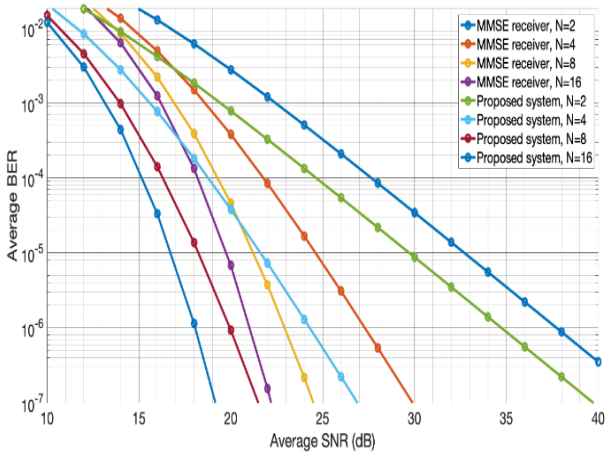

Fig. 11. A comparison between the proposed system's BER and the N channels MMSE receiver's BER at flat Rayleigh fading channel, BW=5.123 MHz, No. of subcarriers=256, rate=35.84 Mbps and Spectral efficiency=6.996 bits/s/Hz.

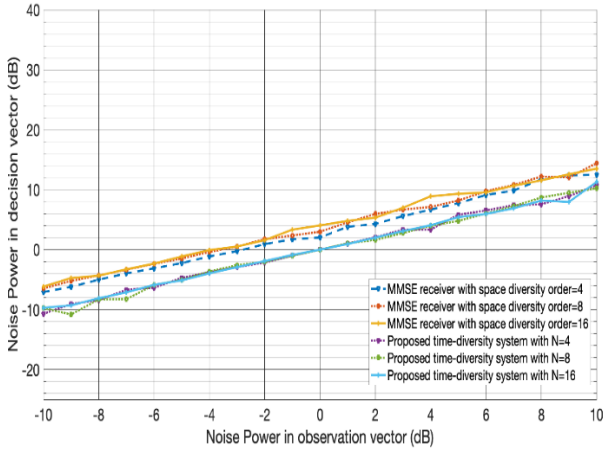

Fig. 12. A comparison between the noise power in the observation vector and the noise power in the decision vector for different configurations of the proposed system and N channel MMSE receiver, BW=5.123 MHz, No. of subcarriers=256, rate=35.84 Mbps and Spectral efficiency=6.996 bits/s/Hz.

Rate is function in symbol rate and number of bits per symbol, the bandwidth is function in roll of factor (α) and the rate symbol. The bandwidth efficiency is equal to the modulation order by 1+α. Figure 13 shows the achievable rate of the proposed system and compared with the theoretical un coded- system. At the same rate, the SNR of the proposed system is higher because of the MIMO used in the proposed system that has residual interference effected on the BER to be less 8×10-8 at the same SNR.

The final performance assessment process uses a real-time system to determine the average BER. The embedded Xilinx FPGA platform is used to implement the proposed system. An MRC receiver is also implemented on the

same platform to compare its performance with the proposed system performance.

The average BER is measured at six averages received SNRs (0 dB, 5 dB, 10 dB, 15 dB, 20 dB, and 25 dB). The real-time BER results of the implemented systems at the smallest Doppler frequency shift are presented in Fig. 13. The results of the real systems almost match to those of the simulated systems. Table II lists the synthesis outcomes of the implementations of the proposed system and the MRC receiver. Because the diversity encoder/decoder and the buffers for interleaving and deinterleaving symbols require more hardware than the conventional system, the complexity of the proposed system is higher than the complexity of the conventional system. The Vitex-7 VC707 Xilinx platform is used (see Fig. 14).

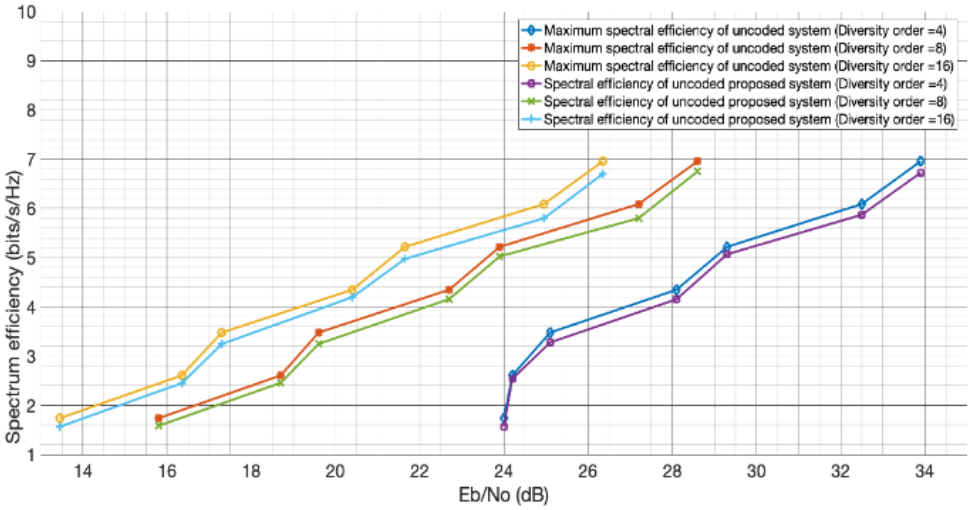

Fig. 13. The achievable rate of uncoded system and the proposed system at different SNR, roll-off factor=0.15 and BER=8×10^{-8}

TABLE II. RESULTS OF THE TIME-DIVERSITY SYSTEM'S IMPLEMENTATION AND THE TRADITIONAL 16-QAM SYSTEM

Resource	Available	The traditional system with MRC receiver and diversity order= 4			The proposed system with time-diversity order= 4		
		Transmitter	Receiver	Utilization %	Transmitter	Receiver	Utilization %
LUT	303,600	76,898	179,431	84.42%	99,533	184,849	93.66%
FF	607,200	115,823	270,174	63.57%	116,238	147,363	95.43%
IO	700	30	42	10.28%	46	67	16.14%
BUFG	32	8	15	71.87%	11	20	96.87%
Worst negative slack		1.781 ns	0.092 ns		0.82 ns	0.0298 ns	
Worst hold slack		0.062ns	0.056 ns		0.039 ns	0.012 ns	

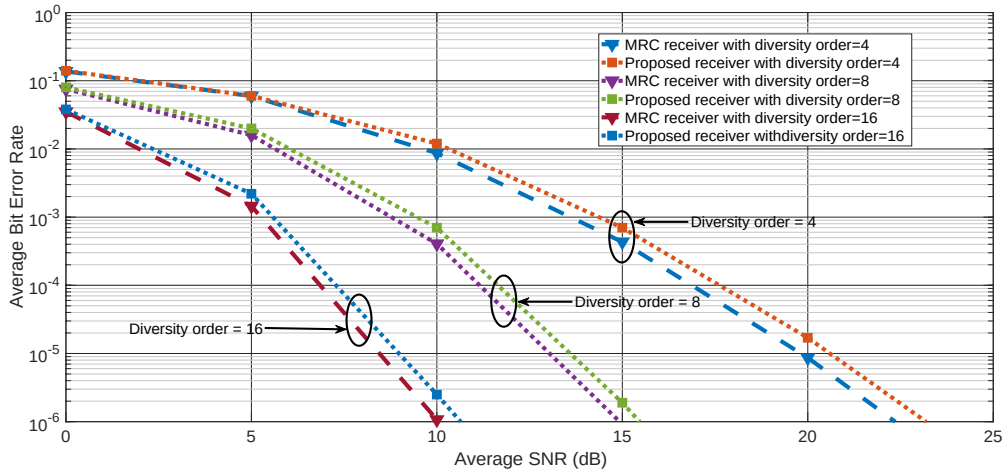

Fig. 14. A comparison between the real-time proposed system's BER and the real-time N channels MRC receiver's BER at flat fading Rayleigh channel with 50 Hz Doppler frequency shift, BW=5.123 MHz, No. of subcarriers=256, rate=35.84 Mbps and Spectral efficiency=6.996 bits/s/Hz.

V. Conclusion

The proposed MIMO-OFDM system achieves time diversity with N order without decreasing the rate of the transmitted symbols or increasing the transmission bandwidth. The proposed system with Walsh matrix diversity encoder/decoder gives the same average BER performance as the MRC receiver. The proposed system achieves the target diversity gain at arbitrary Doppler frequency shift starting from 50 Hz to 7 kHz. The proposed diversity approach in the OFDM system's bandwidth efficiency is equivalent to that of the conventional OFDM system. When MIMO transmission in spatial multiplexing mode is added to the proposed OFDM system, the bandwidth efficiency increases by a factor equivalent to the number of transmitting antennas in the MIMO system. The proposed diversity decoder implicitly merges the modulated symbols in the same way used in the MRC receiver if the diversity encoding process uses a Walsh matrix. The proposed system's time diversity order corresponds to the Walsh matrix's order.

The proposed system's main drawback is the big latency due to the used symbols interleaving and deinterleaving. Moreover, the decorrelator detector, used in the ICI removal stage in the OFDM demodulator, increases the noise power at high Doppler frequency shift cases because of the high correlation between the subcarriers in the OFDM symbols. Another ICI removal method can be used in the future to reduce the noise enhancement done by the decorrelator detector.

Conflict of Interest

The authors declare no conflict of interest.

Author Contributions

Eman and Ashraf conducted the research; Hadia and Abdelhady analyzed the data; Eman and Ashraf wrote the paper; all authors had approved the final version.

References

[1] M. Surendar and P. Muthuchidambaranathan, "Low complexity and high diversity gain non-linear constellation precoded MIMO-OFDM system with subcarrier grouping," *AEU–International Journal of Electronics and Communications*, vol. 70, pp. 265–271, 2016.

[2] K. Y. Seong, L. Simon, G. William, and A. Gareth, "An experimental evaluation of switched combining based macro-diversity for wearable communications operating in an outdoor environment," *IEEE Transactions on Wireless Communications*, Vol. 16, pp. 5338–5352, Aug. 2017.

[3] G. David, G. B. David, V. David, and C. Narcís, "Combined Time, Frequency and Space-diversity in DVB-NGH," *IEEE Transactions on Broadcasting*, vol. 59, pp. 674–684, Dec. 2013.

[4] L. S. Bok, P. Ioannis, C. Sayantan, X. Shugong, and L. Songwu, "Exploiting spatial, frequency, and multiuser diversity in 3GPP LTE cellular networks," *IEEE Transactions on Mobile Computing*, vol. 11, pp. 1652–1665, 2012.

[5] S. Hirofumi, S. Shuhei, M. Tomoki, and M. Fumiaki, "Inter-symbol interference suppression scheme employing periodic signals in coded network MIMO-OFDM systems," *IEEE Radio and Wireless Symposium (RWS)*, 2017.

[6] L. Uowei, L. Yuanan, and X. Xuefang, "Performance analysis of adaptive space-time coded systems with continuous phase modulation", *AEU–International Journal of Electronics and Communications*, Vol. 80, pp. 80–85, 2017.

[7] T. Kannan and E. Kanniga, "Critical review on quality improvement for channel selection in MIMO-OFDM system," *Journal of Critical Reviews*, vol. 7, 2018.

[8] I. M. Nikolaos and D. V. Dimitrios, "A survey on the successive interference cancellation performance for single-antenna and multiple-antenna OFDM systems," *IEEE Communications Surveys and Tutorials*, vol. 4, 2012.

[9] C. Chen, W. Stark, and S. Chen, "Energy-bandwidth efficiency tradeoff in MIMO multi-hop wireless networks," *IEEE J. Sel. Areas Commun*., vol. 29, pp. 1537–1546, Sep. 2011.

[10] F. Heliot, M. A. Imran, and R. Tafazolli, "On the energy efficiency spectral efficiency trade-off over the MIMO Rayleigh fading channel," *IEEE Trans. Communications*, vol. 60, pp. 1345–1356, May 2012.

[11] G. Xiaohu, H. Xi, W. Yuming, C. Min, L. Qiang, H. Tao, and W. C. Xiang, "Energy efficiency optimization for MIMO-OFDM mobile multimedia communication systems with QoS constraints," *IEEE Transactions on Vehicular Technology*, vol. 63, Jun 2014.

[12] A. Yosef and L. Hanzo, "Power versus bandwidth efficiency in wireless communication: The economic perspective," in *Proc. Conference Paper in Vehicular Technology Conference*, IEEE38th, October 2009.

[13] Y. H. Ashraf, "A simple time-space diversity scheme using extended shaping pulse," *Wireless Personal Communications*, pp. 821–841, 2020.

[14] Y. H. Ashraf, "A time diversity scheme with multi-symbol detector for data transmission through flat fading Rayleigh channels," *Physical Communication*, vol. 45, 2021.

[15] H. H. Diana and M. Q. Thuraya, "Effect of doppler shift frequency on the performance of 2×2 OSTBC-OFDM system," *Qalaai Zanist Journal*, vol. 2, pp. 230–238, 2021.

[16] B. Alexis, J. Bruno, andH. Maryline, "Doppler effect reduction in an OFDM system thanks to massive MIMO," *IEEE Access*, vol. 6, pp. 38498–38511, 2018.

[17] S. Ramesh and R. Seshasayanan, "FPGA implemented testbed in 8-by-8 and 2-by-2 OFDM–MIMO channel estimation and design of baseband transceiver," *Springer Plus*, 2016.

[18] S. Ricci and V. Meacci, "FPGA-based doppler frequency Estimator for real-time velocimetry," *Electronics*, vol. 9, 2020.

[19] M. Binkai, K. Matsuda, Y. Yokomura, H. Sano, T. Yoshida, and Y. Konishi, "Real-time doppler-shift compensation in FPGA-based optical transceiver prototype," in *Proc. 2022 27th OptoElectronics and Communications Conference (OECC) and 2022 International Conference on Photonics in Switching and Computing (PSC)*, Toyama, Japan, 2022, pp. 1–4.

[20] Y. H. Ashraf, "Design a new time-diversity system using orthogonal mapping matrix and symbols interleaving for rayleigh flat-fading channels," *IEEE Access*, 2022.

[21] L. A. Dalton and C. N. Georghiades, "A full-rate, full diversity four-antenna quasi-orthogonal space-time block code," *IEEE Transactions on Wireless Communications*, vol. 4, pp. 363–366, 2005.

[22] L. Y. Song and A. G. Burr, "General differential modulation scheme for quasi-orthogonal space--time block codes with partial or full transmit diversity," *IET Communications*, vol. 1, pp. 256–266, April 2007.

[23] A. Y. Hassan, "A frequency-diversity system with diversity encoder and OFDM modulation," *IEEE Access*, vol. 9, pp. 2805–2818, 2021.

[24] T. David and V. Pramod, "Fundamentals of wireless communication," Published in the United States of America by Cambridge University Press, 2005.

[25] S. P. Chester, W. Y. P Eric, J. George, and H. David, "Evolution of uplink MIMO for LTE-advanced," *IEEE Communications Magazine*, vol. 49, February 2011.